

Transient Gas Flow Around Boreholes

DEREK Y. C. CHAN and BARRY D. HUGHES

Department of Mathematics, University of Melbourne, Parkville, Victoria, Australia 3052

LINCOLN PATERSON

CSIRO Division of Geomechanics, PO Box 54, Mount Waverley, Victoria, Australia 3149

(Received: 30 January 1991)

Abstract. We present numerical solutions and analytical approximate solutions to problems of gas flow in porous media arising in the modelling of outbursts in coal mines and the efficient recovery of methane from coal seams.

Key words. Gas flow in porous media, borehole stability, outbursts, methane extraction, coal.

1. Introduction

Fluid flow in a porous solid contributes to the state of stress in the solid. If the fluid is flowing into a borehole or cavity then the fluid flow may contribute to the mechanical failure of that opening. The stress induced by the flow of liquids into boreholes has been studied by Paslay and Cheatham (1963) and Risnes *et al.* (1982), but the stress induced by gas flow does not seem to have received attention. Gas is highly compressible, which provides pressure and stress profiles significantly different from those that occur with liquid flow. The compressibility of gas also means the equation to be solved to describe the flow is highly nonlinear, unlike the linear equation that describes the flow of an incompressible liquid. It is this difficulty that has restricted solutions for gas flow to small pressure changes or other restrictive conditions so that linear approximations can be made. Failure of an underground opening often is associated with dramatic changes in pressure, such as the gas outbursts which occur in coal mines (Paterson, 1986). In these situations, the nonlinearity of the gas flow equation cannot be ignored.

It is our purpose here to provide some approximate solutions which may be used when there are sudden and significant drops of pressure in an underground opening. A knowledge of the pressure profile allows the determination of the effective stress (Jaeger and Cook, 1976) on the porous solid. This may be useful not only for preventing or avoiding failure, but also on those occasions where failure is desired. Such an occasion arises in the creation of cavities for the exploitation of methane occurring naturally in coal. In the coalbed methane completion technology called 'Openhole Cavity Completion' (described in Logan *et al.*, 1989), a coalbed methane well is shut-in so that the pressure in the well approaches the original formation pressure of the coal seam. Then the well is suddenly opened to the

atmosphere resulting in a rapid pressure drop in the well. Coal has been observed to slough into the well on application of this procedure.

In this paper, we examine the pressure distribution induced when a cavity at low pressure p_0 is created in a large (mathematically infinite) porous medium filled with gas at a uniform pressure p_1 . In particular, after a discussion of the fundamental governing equations of the system and their steady-state solutions (Section 2), we obtain numerical solutions for the time-evolution of the pressure for an ideal gas draining into a cavity in a one-dimensional geometry (Section 3). For this geometry, which is most appropriate to the outburst problem, one may seek a similarity solution to reduce the governing partial differential equation to an ordinary differential equation, but as we show in Section 4, accurate numerical solutions are most easily generated by a time-stepping procedure, which has the benefit of being easily generalized to other geometries where similarity solutions are not available. We give in Section 3 a simple argument leading to an analytic approximation for the solution and use this approximation to suggest in Section 4 a phenomenological explicit formula for the solution which fits the numerical data with high precision. In Section 5, we obtain numerical solutions for the time-evolution of the pressure for an ideal gas draining into a cylindrical cavity. An accurate empirical curve for the short-time behaviour of the system is obtained. The similarity between the numerical solutions and the steady-state solutions derived in Section 2 suggests an analytic approximation scheme which leads to simple formulae for the time evolution of the pressure at long times (Section 6). The details of the numerical scheme are contained in an Appendix.

We have ignored additional complications that arise when water is also present, or the permeability of the rock depends on the fluid pressure, or the gas interacts with the rock. These complications arise when methane flows in coal (cf. Paterson, 1990), but it is easier to begin by neglecting these complications. Also, although the basic techniques presented are applicable to general equations of state and general pressure-viscosity relations, we have illustrated them for the specific case of an ideal gas equation of state and a constant shear viscosity.

2. Governing Equations

We recall the fundamental equations governing flow of a gas through a porous material (Muskat 1937). The equation of continuity (mass conservation)

$$\phi \frac{\partial \rho}{\partial t} + \nabla \cdot (\rho \mathbf{q}) = 0 \quad (2.1)$$

relates the superficial velocity or volume flux \mathbf{q} to the mass density ρ and the porosity ϕ . Darcy's law

$$\mathbf{q} = -\frac{k}{\mu} \nabla p, \quad (2.2)$$

couples the superficial velocity to the pressure p in the gas. The constants k and μ are respectively the permeability of the porous material and the shear viscosity of the gas. In Eq. (2.2), we have omitted the effect of gravity, which for the systems to be modelled is unimportant. The pressure and density are coupled by an equation of state. We consider for the present a general equation of state of the form

$$\rho = f(p). \quad (2.3)$$

This equation of state includes as special cases the classic examples of isothermal flow of an ideal gas, in which

$$\rho = Ap, \quad (2.4)$$

where A is inversely proportional to the absolute temperature*, and adiabatic flow of an ideal gas, for which

$$\rho = Bp^{1/\gamma}, \quad (2.5)$$

where B is constant and γ is the familiar ratio of the specific heats.

Equations (2.1) and (2.2) imply that

$$\frac{\partial}{\partial t} f(p) = \nabla \cdot \left\{ \frac{kf(p)}{\mu\phi} \nabla p \right\}. \quad (2.6)$$

It will be convenient to write the equation of state of a general gas in the form

$$\rho = f(p) = Ap/Z(p), \quad (2.7)$$

where A is the temperature-dependent factor in the ideal gas equation of state (2.4). We introduce the *pseudopressure*

$$\psi(p) = 2 \int_0^p \frac{f(p')}{\mu A} dp' = 2 \int_0^p \frac{p'}{\mu Z(p')} dp'. \quad (2.8)$$

Some authors define the pseudopressure with the lower terminal on the integral replaced by the pressure corresponding to a standard state, but for our purposes the definition (2.8) suffices. Equation (2.6) reduces to

$$\frac{\partial}{\partial t} f(p) = \frac{kA}{2\phi} \nabla^2 \psi(p). \quad (2.9)$$

If we note that

$$\frac{\partial \psi}{\partial t} = \frac{2f(p)}{\mu A} \frac{\partial p}{\partial t} = \frac{2}{\mu Ac(\psi)} \frac{\partial}{\partial t} f(p), \quad (2.10)$$

*If ρ is measured in gm cm⁻³ and p in dyne cm⁻², N_A = Avogadro's number = 6.02×10^{23} , T is the absolute temperature and k_B = Boltzmann's constant = 1.38×10^{-16} erg K⁻¹, then A = molecular weight in gm mole⁻¹/($N_A k_B T$).

where

$$c(\psi) = \frac{1}{\rho} \frac{d}{d\rho} f(p) = \frac{1}{\rho} \frac{d\rho}{dp} \quad (2.11)$$

is the compressibility, Equation (2.9) can be formally rewritten as a nonlinear differential equation for the pseudopressure, viz.

$$\frac{\partial \psi}{\partial t} = \frac{k}{\mu \phi c(\psi)} \nabla^2 \psi. \quad (2.12)$$

In some contexts, the gas viscosity μ may need to be allowed to be a function of the pseudopressure. We shall not consider such cases here.

Steady solutions (i.e. solutions in which the pressure is constant in time) are easily deduced by solving Laplace's equation

$$\nabla^2 \psi = 0. \quad (2.13)$$

The three simple solutions given below describe the flow of a gas in a porous material bounded by surfaces at which the pressure is prescribed. These three solutions are the starting point for analytic approximate solutions for some time-dependent problems, as discussed in Section 6.

(i) *One-dimensional steady solutions*

With x a spatial coordinate, Equation (2.13) reduces to $d^2\psi/dx^2 = 0$, and so ψ is a linear function of x . If we apply the boundary conditions

$$p = p_0 \quad \text{at } x = 0 \quad \text{and} \quad p = p_1 \quad \text{at } x = X > 0, \quad (2.14)$$

we have

$$\psi(p) = \psi(p_0) + [\psi(p_1) - \psi(p_0)]x/X. \quad (2.15)$$

(ii) *Radially symmetric two-dimensional steady solutions*

With r a radial coordinate, Equation (2.13) reduces to $d^2\psi/dr^2 + r^{-1} d\psi/dr = 0$, and so ψ is a linear combination of 1 and $\log r$. If we apply the boundary conditions

$$p = p_0 \quad \text{at } r = a \quad \text{and} \quad p = p_1 \quad \text{at } r = R > a, \quad (2.16)$$

we have

$$\psi(p) = \psi(p_0) + [\psi(p_1) - \psi(p_0)] \frac{\log(r/a)}{\log(R/a)}. \quad (2.17)$$

(iii) *Radially symmetric three-dimensional steady solutions*

With r a radial coordinate, Equation (2.13) reduces to $d^2\psi/dr^2 + 2r^{-1} d\psi/dr = 0$, and so ψ is a linear combination of 1 and r^{-1} . If we apply the boundary conditions

$$p = p_0 \quad \text{at } r = a \quad \text{and} \quad p = p_1 \quad \text{at } r = R > a, \quad (2.18)$$

we have

$$\psi(p) = \frac{R\psi(p_1) - a\psi(p_0)}{R - a} - \frac{aR[\psi(p_1) - \psi(p_0)]}{(R - a)r}. \quad (2.19)$$

In all cases, the pressure p is determined in terms of the pseudopressure ψ , defined by Equation (2.8). In dimensions 1, 2 and 3, ψ is linear in the variables x , $\log r$ and $1/r$, respectively. We shall exploit this observation in deriving simple analytic approximate solutions for large time in Section 6. It may be noted here for later reference that for the ideal gas equation of state,

$$c(\psi) = 1/p \quad \text{and} \quad \psi(p) = p^2/\mu. \quad (2.20)$$

3. Similarity Solutions in One Dimension

It may be noted here that the one-dimensional time-dependent problem may be solved exactly for some special equations of state. The situation is an exact parallel of the non-linear diffusion problem addressed by Philip (1960). Equation (2.12) reduces in one dimension to

$$\frac{\partial \psi}{\partial t} = \frac{k}{\mu \phi c(\psi)} \frac{\partial^2 \psi}{\partial x^2}. \quad (3.1)$$

The absence of any geometrical length scale suggests that we seek a solution in which x is scaled with a length constructed from the time and the other physical parameters of the problem. We write

$$\xi = x/X(t), \quad (3.2)$$

where

$$X(t) = \left\{ \frac{kA[\psi(p_1) - \psi(p_0)]t}{\phi f(p_1)} \right\}^{1/2}. \quad (3.3)$$

The significance of the choice of the prefactor in Equation (3.3) will become apparent in Section 6. It is easily shown that

$$\frac{d^2 \psi}{d\xi^2} + \frac{\mu c(\psi)A[\psi(p_1) - \psi(p_0)]}{2f(p_1)} \xi \frac{d\psi}{d\xi} = 0. \quad (3.4)$$

This equation is to be solved subject to the boundary conditions

$$\psi(p) = \psi(p_0) \quad \text{at} \quad \xi = 0 \quad \text{and} \quad \psi(p) \rightarrow \psi(p_1) \quad \text{as} \quad \xi \rightarrow \infty. \quad (3.5)$$

In the nonlinear diffusion literature, the problem has sometimes been addressed by what amounts to searching for equations of state which make Equation (3.4) solvable in terms of known functions. In contrast, we address here the approximate solution of Equation (3.4) for equations of state of physical interest. We illustrate this with the case of an ideal gas, with $p_0 = 0$, but the reader will readily see that the

approach is easily generalized to accommodate other equations of state and nonzero pressure p_0 at $\xi = 0$. For problems of gas flow in coal, $p_0 \ll p_1$, so the neglect of p_0 is usually reasonable. We write

$$\psi = \Psi p_1^2 / \mu. \quad (3.6)$$

Using Equations (2.20) and (3.6), we find that Equation (3.4) becomes

$$\frac{d^2\Psi}{d\xi^2} + \frac{\xi}{2\sqrt{\Psi}} \frac{d\Psi}{d\xi} = 0, \quad (3.7)$$

with boundary conditions

$$\Psi(p) = 0 \quad \text{at } \xi = 0 \quad \text{and} \quad \Psi(p) \rightarrow 1 \quad \text{as } \xi \rightarrow \infty. \quad (3.8)$$

For large values of ξ , where Ψ is close to 1, we may replace Equation (3.7) by

$$\frac{d^2\Psi}{d\xi^2} + \frac{\xi}{2} \frac{d\Psi}{d\xi} = 0, \quad (3.9)$$

so that

$$\frac{d}{d\xi} \left\{ \exp(\xi^2/4) \frac{d\Psi}{d\xi} \right\} = 0. \quad (3.10)$$

The solution of this equation can be expressed in terms of the error function

$$\operatorname{erf}(z) = \frac{2}{\sqrt{\pi}} \int_0^z \exp(-u^2) du, \quad (3.11)$$

but the important thing to note here is that for large ξ , $1 - \Psi$ contains the rapidly decaying factor $\exp(-\xi^2/4)$.

If we write

$$\Psi = 1 - \exp[-\Phi(\xi)], \quad (3.12)$$

the differential equation (3.9) becomes

$$\Phi'' - (\Phi')^2 + \frac{\xi \Phi'}{2[1 - \exp(-\Phi)]^{1/2}} = 0. \quad (3.13)$$

We attempt a solution of the form

$$\Phi(\xi) = a\xi + b\xi^2 + \dots \quad (3.14)$$

For small ξ , the differential equation (3.13) leads to the requirement that

$$2b = a^2. \quad (3.15)$$

Since we require $\Phi(\xi) \sim \xi^2/4$ as $\xi \rightarrow \infty$, if we make the choice

$$a = 1/\sqrt{2} \cong 0.707 \quad \text{and} \quad b = 1/4, \quad (3.16)$$

the trial solution is consistent for $\xi \rightarrow 0$ and for $\xi \rightarrow \infty$, although we have no guarantee that it will be reasonable for $\xi \cong 1$, so we tentatively propose that

$$\Psi \cong 1 - \exp(-\xi/\sqrt{2} - \xi^2/4). \quad (3.17)$$

For different equations of state, the same approach goes through, although different numerical values of a and b are obtained. The numerical performance of Equation (3.17) is addressed in Section 4.

4. Numerical Solutions in One Dimension

We have obtained numerical solutions for transient one-dimensional flow of an ideal gas in one dimension. In most practical calculations, the pressure in the well (typically 1 atmosphere) is far less than the pressure deep inside the porous medium (typically 40–60 atmospheres), so we have considered only the case in which the well pressure p_0 is zero, while the pressure far from the well is $p_1 > 0$. For the ideal gas equation of state, using Equations (2.20), the partial differential equation (2.12) becomes

$$\frac{\partial \psi}{\partial t} = \frac{k\psi^{1/2}}{\phi\mu^{1/2}} \frac{\partial^2 \psi}{\partial x^2}. \quad (4.1)$$

It is convenient to introduce dimensionless variables by writing

$$\psi = \frac{p_1^2}{\mu} \Psi, \quad t = t_0 \tau \quad \text{and} \quad x = x_0 z, \quad (4.2)$$

where x_0 and t_0 are length and time scales, respectively. The dimensionless version of Equation (4.1) is

$$\frac{\partial \Psi}{\partial \tau} = \varepsilon \Psi^{1/2} \frac{\partial^2 \Psi}{\partial z^2}, \quad (4.3)$$

where

$$\varepsilon = \frac{kp_1 t_0}{x_0^2 \phi \mu}. \quad (4.4)$$

The appearance of the time and length scales as t_0/x_0^2 in the dimensionless parameter ε reflects the existence of a similarity solution for this system. Since we are able to choose x_0 and t_0 at our discretion, we may henceforth assume that

$$\varepsilon = 1. \quad (4.5)$$

The boundary conditions to be applied are $\Psi = 0$ at $z = 0$ and $\Psi \rightarrow 1$ as $z \rightarrow \infty$.

Equation (4.3) is solved by the implicit time-stepping method described in the Appendix. In Figure 1 we show Ψ as a function of ξ , where

$$\xi^2 = \frac{z^2}{\tau} = \frac{\phi \mu x^2}{kp_1 t}. \quad (4.6)$$

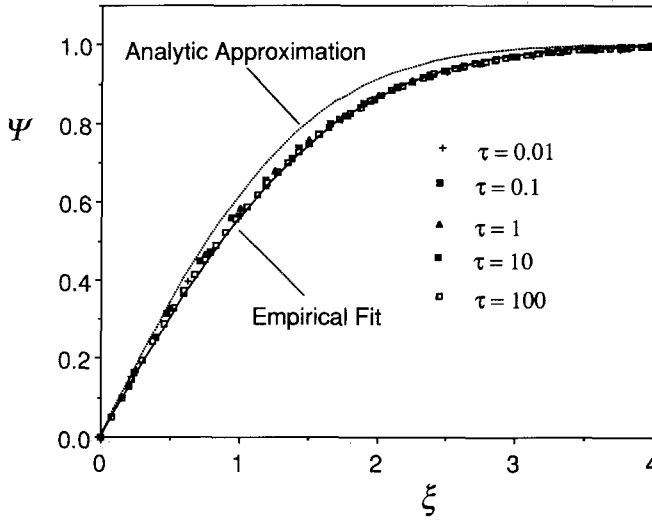


Fig. 1. Numerical solution for the dimensionless pseudopressure Ψ for one dimensional flow of ideal gas into a cavity at zero pressure. Here $\Psi = \mu\psi/p_1^2 = p^2/p_1^2$, where p_1 is the pressure far from the cavity and $\xi = z/\tau^{1/2} = \{\phi\mu x^2/(kp_1 t)\}^{1/2}$. The solutions for different times lie on a common curve. The analytic approximate solution (3.17) and the empirical approximate solution (4.7) are also shown. For practical purposes, the latter is indistinguishable from the numerical solutions.

for several different dimensionless times τ . These solutions for different times fall on a single curve, which represents the similarity solution discussed in Section 3. It is actually simpler to obtain the similarity solution by timestepping and plotting the solution as a function of ξ than by solving the differential equation (3.9).

The analytic approximate solution (3.17) is included in Figure 1. It fits the numerical data reasonably well, with the worst error (less than 10%) occurring for $\xi \cong 2$. We have also obtained an empirical equation for the solution, viz.

$$\Psi = 1 - e^{-(0.625\xi + 0.186\xi^2)}, \quad (4.7)$$

which is also shown in Figure 1. The empirical solution, which has a correlation coefficient in excess of 0.999, is for all practical engineering purposes the solution of the problem.

5. Numerical Solutions for a Cylindrical Well

We have obtained numerical solutions for transient flow of an ideal gas into a cylindrical well. As the pressure in the well (typically 1 atmosphere) is far less than the pressure deep inside the porous medium (typically 40–60 atmospheres), we have only considered the case in which the well pressure p_0 is zero, while the pressure far from the well is $p_1 > 0$. The radius of the well is denoted by a . For the ideal gas

equation of state, Equations (2.12) and (2.20) give

$$\frac{\partial \psi}{\partial t} = \frac{k\psi^{1/2}}{\phi\mu^{1/2}} \nabla^2 \psi. \quad (5.1)$$

We exploit the radial geometry by writing $z = \log(r/a)$ to give

$$\frac{\partial \psi}{\partial t} = \frac{k\psi^{1/2}}{\phi a^2 \mu^{1/2}} e^{-2z} \frac{\partial^2 \psi}{\partial z^2}. \quad (5.2)$$

It is convenient to introduce dimensionless variables by writing

$$\psi = \frac{p_1^2}{\mu} \Psi \quad \text{and} \quad t = t_0 \tau, \quad (5.3)$$

where

$$t_0 = \frac{\phi \mu a^2}{k p_1}. \quad (5.4)$$

For methane ($\mu \cong 10^{-5}$ Pa s, $p_1 \cong 5 \times 10^6$ Pa) leaking into a typical well-bore ($a \cong 0.1$ m) from a coal seam ($k \cong 1$ milliDarcy = 10^{-15} m², $\phi \cong 0.04$), the characteristic time is

$$t_0 \cong 0.8 \text{ sec.} \quad (5.5)$$

If we increase a to mineshaft diameters ($a \cong 1$ m), t_0 is increased to 80 sec.

Equation (5.2) becomes

$$\frac{\partial \Psi}{\partial \tau} = e^{-2z} \Psi^{1/2} \frac{\partial^2 \Psi}{\partial z^2}, \quad (5.6)$$

to be solved with boundary conditions $\Psi = 0$ at $z = 0$ and $\Psi \rightarrow 1$ as $z \rightarrow \infty$.

The solution is constructed by an implicit time-stepping method described in the Appendix. In Figure 2 we show Ψ as a function of z for several different times. It may be observed that the solution is linear over a substantial interval, so that at each fixed time the solution is qualitatively rather similar to the steady-state solution given by Equation (2.17). We exploit this observation in Section 6.

For small enough times, the pseudopressure Ψ has decayed appreciably only in a region of small thickness compared to the well diameter, so the solution for the pseudopressure should be indistinguishable from that for a one-dimensional geometry, with $x = r - a$. As noted in Section 3, in the one-dimensional geometry, the absence of any natural length scale forces the solution to be a function of $x/t^{1/2}$. Thus, if for each value of τ , we plot Ψ as a function of

$$\zeta = (r/a - 1)/\tau^{1/2} = (e^z - 1)/\tau^{1/2}, \quad (5.7)$$

the curves for different small values of τ should lie on top of each other. That this is so in practice is demonstrated in Figure 3, where data for two different values of

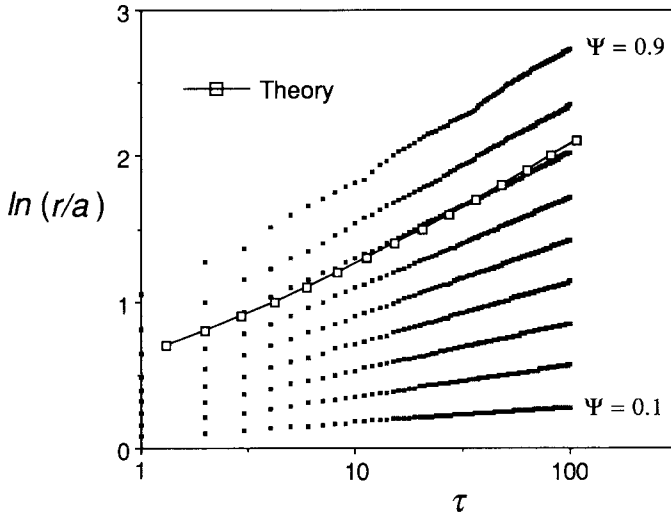


Fig. 2. Numerical solution for the dimensionless pseudopressure Ψ for flow of ideal gas into a cylindrical cavity at zero pressure. We show the time evolution of curves of constant Ψ for $\Psi = 0.1$ to 0.9 in steps of 0.1 . The continuous curve marked with open squares represents the location of the fictitious moving interface (specified by Equation (6.16)) which is used to construct the analytic approximate solution in Section 6.

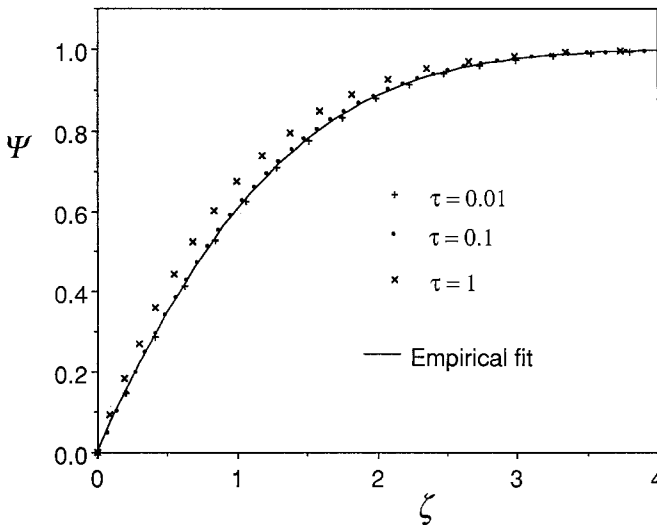


Fig. 3. Small time numerical solution for the dimensionless pseudopressure Ψ for flow of ideal gas into a cylindrical cavity at zero pressure. The dimensionless variable ζ is defined by Equation (5.7). The empirical approximate solution (5.8) is also shown.

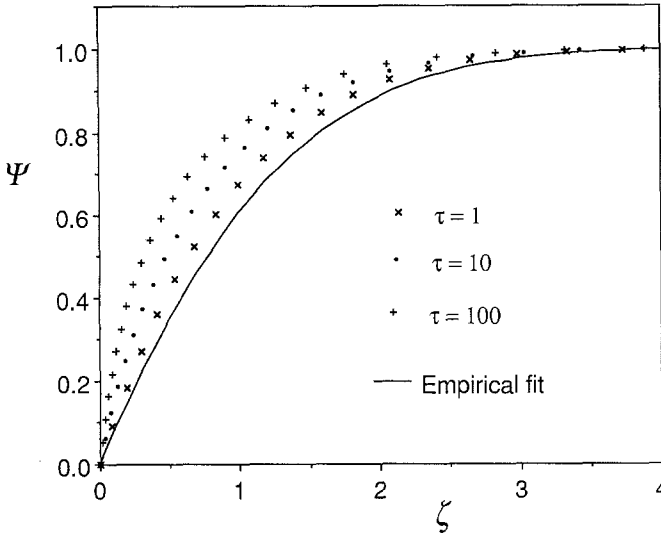


Fig. 4. Large time numerical solution for the dimensionless pseudopressure Ψ for flow of ideal gas into a cylindrical cavity at zero pressure. The dimensionless variable ζ is defined by Equation (5.7). The empirical approximate solution (5.8) is also shown.

τ is shown. We have obtained an empirical equation for this curve, viz.

$$\Psi = 1 - e^{-(0.776\zeta + 0.152\zeta^2)} \tag{5.8}$$

This curve is also shown in Figure 3. It fits the numerical solutions for $\tau \leq 0.1$ with a correlation coefficient of 0.999. For larger times, the curves for Ψ as a function of ζ are displaced from the small-time universal curve as shown in Figure 4.

6. Approximate Analytic Solutions for Large Time

The numerical solutions reported in Section 5 above show that at a given time, the pressure p rises from p_0 at the well surface to pressure p_1 over a region, the width of which increases with time. The form of $\psi(p)$ over this region is similar to the steady-state solution derived in Section 2. We now use this observation to construct approximate analytic solutions for large times. Our fundamental approximation is very easily explained. We assume that there is a ‘dividing surface’ in the porous material. Between the dividing surface and the well, the pressure distribution is approximated by the pressure distribution for steady flow. Beyond the dividing surface, the gas is assumed stationary and at pressure p_1 . The dividing surface recedes from the well as the gas escapes. The position of the dividing surface is located by an analogue of the boundary condition found in the well-known Stefan problems of heat conduction (Crank, 1984). If \mathbf{n} denotes the normal to the dividing surface and \mathbf{v} is the velocity of the dividing surface, then

$$\phi \rho \mathbf{v} \cdot \mathbf{n} = -\rho \mathbf{q} \cdot \mathbf{n} \tag{6.1}$$

This equation asserts that gas brought into motion as the dividing surface recedes is carried away by the usual pressure-gradient driven transport law.

From Equations (6.1) and (2.2), we deduce that

$$\mathbf{v} \cdot \mathbf{n} = \frac{k}{\mu\phi} \nabla p \cdot \mathbf{n} = \frac{kA}{2\phi f(p)} \nabla\psi \cdot \mathbf{n}, \quad (6.2)$$

where the gradient is evaluated at the dividing surface. In simple geometries, such as those now to be considered, the combination of the steady-state formula for the pseudopressure and Equation (6.2) produces an ordinary differential equation, the solution of which locates the dividing surface. The initial condition for the problem is that at time $t = 0$, the dividing surface coincides with the well, which is held at pressure p_0 . The mass flux $J(t)$ into the well is given by the normal component of $(\rho k/\mu)\nabla p = (kA/2)\nabla\psi$ at the wall of the well.

(i) *One-dimensional approximate solutions.* With x a spatial coordinate, the well corresponding to $x = 0$ and the dividing surface to $x = X(t)$, we have from Equation (2.15)

$$\psi(p) = \psi(p_0) + [\psi(p_1) - \psi(p_0)]x/X(t). \quad (6.3)$$

Equation (6.2) reduces to

$$\frac{dX}{dt} = \frac{kA[\psi(p_1) - \psi(p_0)]}{2\phi f(p_1)X(t)}. \quad (6.4)$$

This equation is to be solved subject to the initial condition

$$X(0) = 0. \quad (6.5)$$

The appropriate solution is evidently

$$X(t) = \left\{ \frac{kA[\psi(p_1) - \psi(p_0)]t}{\phi f(p_1)} \right\}^{1/2}. \quad (6.6)$$

If we consider the one-dimensional model as representing the case when the well is a half-space (i.e. infinite, with a plane interface), the mass flux into the well per unit area of wall is

$$J(t) = \frac{kA[\psi(p_1) - \psi(p_0)]}{2X(t)} = \left\{ \frac{kA[\psi(p_1) - \psi(p_0)]\phi f(p_1)}{4t} \right\}^{1/2}. \quad (6.7)$$

It may be noted here that the introduction of the variable $\xi = x/X(t)$, as used in our discussion of similarity solutions in Section 3, enables the approximate solution to be written in the form

$$\psi(p) \cong \begin{cases} \psi(p_0) + [\psi(p_1) - \psi(p_0)]\xi, & 0 \leq \xi \leq 1, \\ \psi(p_1), & \xi \geq 1. \end{cases} \quad (6.8)$$

For the special case of an ideal gas, with $p_0 = 0$ and $\Psi = \psi p_0^2 / \mu$, this simplifies to

$$\Psi = \begin{cases} \xi, & 0 \leq \xi \leq 1 \\ 1, & \xi \geq 1 \end{cases}. \tag{6.9}$$

Inspection of Figure 1 will show that the fit is rather poor, but fortunately we already have a reasonable analytic approximation (Equation (3.17)) and an excellent numerical fit (Equation (4.7)).

(ii) *Radially symmetric two-dimensional approximate solutions.* With r a radial coordinate, the well corresponding to $r = 0$ and the dividing surface to $r = R(t)$, we have from Equation (2.17)

$$\psi(p) = \psi(p_0) + [\psi(p_1) - \psi(p_0)] \frac{\log(r/a)}{\log(R(t)/a)}. \tag{6.10}$$

Equation (6.2) reduces to

$$\frac{dR}{dt} = \frac{kA[\psi(p_1) - \psi(p_0)]}{2\phi f(p_1) \log(R(t)/a)R(t)}. \tag{6.11}$$

This equation is to be solved subject to the initial condition

$$R(0) = a. \tag{6.12}$$

Equation (6.11) can be transformed into an equation for

$$S(t) = [R(t)/a]^2, \tag{6.13}$$

viz.

$$\log S \frac{dS}{dt} = \alpha, \tag{6.14}$$

where $S(0) = 1$ and

$$\alpha = \frac{2kA[\psi(p_1) - \psi(p_0)]}{a^2\phi f(p_1)}. \tag{6.15}$$

For the special case of an ideal gas with $p_0 = 0$, we have $\alpha = 2/t_0$, where t_0 is defined by Equation (5.4). The appropriate solution is

$$S(t) \log S(t) - S(t) = \alpha t - 1. \tag{6.16}$$

For small t , we write $S(t) = 1 + \varepsilon(t)$, where $\varepsilon(t) \ll 1$, and Equation (6.16) implies that as $t \rightarrow 0$, $\varepsilon(t)^2 \sim 2\alpha t$, so that

$$\frac{R(t)}{a} = 1 + \frac{\sqrt{(\alpha t)}}{\sqrt{2}} + \dots \text{ as } t \rightarrow 0. \tag{6.17}$$

For large t , standard asymptotic techniques (cf. Olver (1974), p. 12) show that

$$\frac{R(t)}{a} \sim \frac{(\alpha t)^{1/2}}{[\log(\alpha t)]^{1/2}} \quad \text{as } t \rightarrow \infty. \quad (6.18)$$

The mass flux into the well per unit area of wall is

$$J(t) = \frac{kA[\psi(p_1) - \psi(p_0)]}{2a \log(R(t)/a)} = \frac{\alpha a \phi f(p_1)}{4 \log(R(t)/a)}. \quad (6.19)$$

Using the asymptotic form (6.17), we infer that

$$J(t) \sim \left\{ \frac{kA[\psi(p_1) - \psi(p_0)]\phi f(p_1)}{4t} \right\}^{1/2} \quad \text{as } t \rightarrow 0, \quad (6.20)$$

so the initial flux is exactly the same as that for the one-dimensional problem. This to be expected, since at small times, the dominant gas motion occurs so close to the wall of the well that the effect of curvature is not seen. For large times, we find from Equation (6.18) that to leading order,

$$J(t) \sim \frac{\alpha a \phi f(p_1)}{2 \log(\alpha t)}. \quad (6.21)$$

(iii) *Radially symmetric three-dimensional approximate solutions.* We have not constructed numerical solutions for the case of gas draining into a spherical cavity, since this problem is less relevant to the applications we have in mind, but for completeness we briefly discuss analytic approximate solutions for this case. With r a radial coordinate, the well corresponding to $r = a$ and the dividing surface to $r = R(t)$, we have from Equation (2.19)

$$\psi(p) = \frac{R(t)\psi(p_1) - a\psi(p_0)}{R(t) - a} - \frac{aR(t)[\psi(p_1) - \psi(p_0)]}{[R(t) - a]r}. \quad (6.22)$$

Equation (6.2) reduces to

$$\frac{dR}{dt} = \frac{kAa[\psi(p_1) - \psi(p_0)]}{2\phi f(p_1)R(t)[R(t) - a]} = \frac{a^3\alpha}{4R(t)[R(t) - a]}, \quad (6.23)$$

to be solved subject to the initial condition

$$R(0) = a. \quad (6.24)$$

The solution is

$$\frac{R(t)^3}{3} - \frac{aR(t)^2}{2} + \frac{a^3}{6} = \frac{a^3\alpha t}{4}. \quad (6.25)$$

The asymptotic analysis of the solution for small and large t is straightforward. With α as defined by Equation (6.15), we find that

$$\frac{R(t)}{a} = 1 + \frac{\sqrt{(\alpha t)}}{\sqrt{2}} + \dots \quad \text{as } t \rightarrow 0 \quad (6.26)$$

(cf. Equation (6.17) for the two-dimensional case) and

$$\frac{R(t)}{a} \sim \left\{ \frac{3\alpha t}{4} \right\}^{1/3} \quad \text{as } t \rightarrow \infty. \tag{6.27}$$

For small times the asymptotic form of the mass flux into the well coincides with that for the one-dimensional case. It is easily shown that

$$J(t) \rightarrow \frac{a\alpha\phi f(p_1)}{4} \quad \text{as } t \rightarrow \infty. \tag{6.28}$$

It may be noted that for a given dimension, the qualitative forms of the equation locating the dividing surface and the equation of the mass flux into the well are independent of the details of the equation of state connecting the pressure and density.

Appendix. The Numerical Scheme

In Sections 4 and 5, we are faced with the numerical solution of equations of the form

$$\frac{\partial \Psi}{\partial \tau} = F(z, \Psi) \frac{\partial^2 \Psi}{\partial z^2}, \tag{A.1}$$

with boundary conditions $\Psi = 0$ at $z = 0$ and $\Psi \rightarrow 1$ as $z \rightarrow \infty$. In Section 4,

$$F(z, \Psi) = \Psi^{1/2}, \tag{A.2}$$

while in Section 5,

$$F(z, \Psi) = e^{-2z}\Psi^{1/2}. \tag{A.3}$$

Equation (A.1) is solved by an implicit time-stepping method. With Ψ_i^j denoting the dimensionless pseudopressure at $z_i = i\Delta z$ and dimensionless time $\tau_j = j\Delta \tau$, the partial derivatives are approximated by

$$\frac{\partial \Psi}{\partial \tau} \cong (\Psi_i^{j+1} - \Psi_i^j) / \Delta \tau \tag{A.4}$$

and

$$\frac{\partial^2 \Psi}{\partial z^2} \cong (\Psi_{i+1}^{j+1} - 2\Psi_i^{j+1} + \Psi_{i-1}^{j+1}) / (\Delta z)^2. \tag{A.5}$$

The partial differential equation is therefore replaced by the tridiagonal system of nonlinear equations

$$-\beta_i \Psi_{i-1}^{j+1} + (1 + 2\beta_i) \Psi_i^{j+1} - \beta_i \Psi_{i+1}^{j+1} = \Psi_i^j, \tag{A.6}$$

where

$$\beta_i = F(z_i, \Psi_i^{j+1}) \frac{\Delta\tau}{(\Delta z)^2}. \quad (\text{A.7})$$

For each time $\tau_j = j\Delta\tau$, we use an iterative scheme to determine the solution at time $\tau_{j+1} = (j+1)\Delta\tau$. We use an initial estimate for Ψ_i^{j+1} to calculate the coefficients β_i and then Equation (A.6) is taken as a linear tridiagonal system from which we can determine a better estimate of Ψ_i^{j+1} and hence a better estimate of β_i . This procedure, which is stable and rapidly convergent, is repeated at each timestep, until the desired accuracy for Ψ_i^{j+1} is obtained.

References

- Crank, J., 1984, *Free and Moving Boundary Problems*, Oxford University Press.
- Jaeger, J. C. and Cook, N. G. W., 1976, *Fundamentals of Rock Mechanics*, 2nd edn., p. 219, Chapman and Hall, London.
- Logan, T. L., Clark, W. F., and McBane, R. A., 1989, Comparing different coalbed methane completion techniques, hydraulic fracture and openhole cavity, at the Northeast Blanco Unit, San Juan Basin, *Proc. Coalbed Methane Symposium*, Tuscaloosa, Alabama, April 17–20.
- Muskat, M., 1937, *The Flow of Homogeneous Fluids Through Porous Media*, McGraw-Hill, New York.
- Olver, F. W. J., 1974, *Asymptotics and Special Functions*, Academic Press, New York.
- Paslay, P. R. and Cheatham, J. B., 1963, Rock stresses induced by flow of fluids into boreholes, *Soc. Petrol. Engrs. J.* **3**, 85–94.
- Paterson, L., 1986, A model for outbursts in coal, *Int. J. Rock Mech. Min. Sci. & Geomech. Abstr.* **23**, 327–332.
- Paterson, L., 1990 (ed.), *Methane Drainage from Coal*, Proc. Workshop, Syndal, Victoria, CSIRO Division of Geomechanics.
- Philip, J. R., 1960, General method of exact solution of the concentration-dependent diffusion equation, *Australian J. Phys.* **13**, 1–12.
- Risnes, R., Bratti, R. K., and Horsrud, P., 1982, Sand stresses around a wellbore, *Soc. Petrol. Engrs. J.* **22**, 883–898.